

# 离子氮铝共渗方法及对 42CrMo 钢组织性能的影响

康前飞<sup>1a,2</sup>, 杨卫民<sup>1b,3</sup>, 魏坤霞<sup>1a,2</sup>, 汪丹丹<sup>1a,1b</sup>, 刘细良<sup>1a,1b</sup>, 胡静<sup>1a,1b,2</sup>

(1.常州大学 a.江苏省材料表面科学与技术重点实验室 b.材料科学与工程国家级实验教学示范中心, 江苏 常州 213164; 2.常州大学 怀德学院, 江苏 靖江 214500; 3.常州赛斐斯新材料科技有限公司, 江苏 常州 213164)

**摘要:** **目的** 研发离子氮铝共渗试验方法, 达到不影响 42CrMo 钢基体组织性能前提下, 显著提高试样表面硬度和耐磨性效果。**方法** 采用电解法在 42CrMo 钢表面沉积氢氧化铝膜, 再在 520 °C/4 h 工艺下进行离子氮铝共渗处理, 并在相同工艺参数条件与传统离子渗氮进行对比。用光学显微镜、维氏显微硬度计、摩擦磨损测试机、X 射线衍射仪及 SEM 对截面显微组织、截面硬度、耐磨性及物相等进行了测试和分析。**结果** 获得了离子氮铝共渗试验方法, 在 520 °C/4 h 相同工艺参数下, 离子氮铝共渗形成的化合物层和有效硬化层厚度比常规离子渗氮显著增加, 其中, 化合物层厚度由 17.24 μm 增加到 52.13 μm, 有效扩散层从 175 μm 增加到 1 050 μm, 相当于等离子处理效率提升 6 倍; 同时, 渗层形成了 AlN 及 Fe<sub>x</sub>Al 强化相, 大幅度提高了渗层的硬度及耐磨性能。表面硬度由 750HV0.025 提高到 1 250HV0.025, 摩擦因数由常规离子渗氮 0.52 下降到 0.29, 磨损率由常规离子渗氮 3.22×10<sup>-5</sup> g/(m·N) 下降到 1.21×10<sup>-5</sup> g/(m·N), 磨痕明显减轻。**结论** 采用电解硝酸铝生成氢氧化铝沉淀附着在工件表面作为预处理, 获得了离子氮铝共渗试验方法, 与常规离子渗氮相比, 离子氮铝共渗形成了多层次渗层结构, 大幅度提高常规离子处理效率、表面硬度及耐磨性。

**关键词:** 42CrMo 钢; 离子渗氮; 氮铝共渗; 耐磨性; 摩擦因数; 电沉积

**中图分类号:** TG156.8+2 **文献标识码:** A **文章编号:** 1001-3660(2023)01-0394-07

**DOI:** 10.16490/j.cnki.issn.1001-3660.2023.01.040

## Development of a Novel Plasma Aluminum-nitriding Methodology and Its Effect on the Microstructure and Properties for 42CrMo Steel

KANG Qian-fei<sup>1a,2</sup>, YANG Wei-min<sup>1b,3</sup>, WEI Kun-xia<sup>1a,2</sup>, WANG Dan-dan<sup>1a,1b</sup>,  
LIU Xi-liang<sup>1a,1b</sup>, HU Jing<sup>1a,1b,2</sup>

(1. a. Jiangsu Key Laboratory of Materials Surface Science and Technology, b. National Experimental Demonstration

收稿日期: 2021-12-24; 修订日期: 2022-04-09

Received: 2021-12-24; Revised: 2022-04-09

**基金项目:** 国家自然科学基金 (21978025、51774052); 江苏省第三期优势学科建设项目 (PAPD-3); 江苏高校品牌专业建设工程资助项目 (TAPP); 常州科技项目 (CJ20210114); 江苏省研究生创新基金项目 (CX10292)

**Fund:** The National Natural Science Foundation of China (21978025, 51774052); Priority Academic Program Development of Jiangsu Higher Education Institutions (PAPD-3); Top-notch Academic Program Projects of Jiangsu Higher Education Institutions (TAPP); Science and Technology Project of Changzhou City (CJ20210114); Postgraduate Research & Practice Innovation Program of Jiangsu Province (CX10292)

**作者简介:** 康前飞 (1997—), 男, 硕士研究生, 主要研究方向为表面工程。

**Biography:** KANG Qian-fei (1997-), Male, Postgraduate, Research focus: surface engineering.

**通讯作者:** 胡静 (1966—), 女, 博士, 教授, 主要研究方向为金属材料表面改性。

**Corresponding author:** HU Jing (1966-), Female, Ph. D., Professor, Research focus: surface modification for metals.

**引文格式:** 康前飞, 杨卫民, 魏坤霞, 等. 离子氮铝共渗方法及对 42CrMo 钢组织性能的影响[J]. 表面技术, 2023, 52(1): 394-400.

KANG Qian-fei, YANG Wei-min, WEI Kun-xia, et al. Development of a Novel Plasma Aluminum-nitriding Methodology and Its Effect on the Microstructure and Properties for 42CrMo Steel[J]. Surface Technology, 2023, 52(1): 394-400.

Center for Materials Science and Engineering, Changzhou University, Jiangsu Changzhou 213164, China;

2. Huaide College, Changzhou University, Jiangsu Jingjiang 214500, China;

3. Changzhou Surface Advanced Materials Technology Co., Ltd., Jiangsu Changzhou 213164, China)

**ABSTRACT:** Plasma nitriding is a widely used environment friendly chemical heat treatment, which can effectively improve the surface layer hardness, wear resistance and corrosion resistance of metal components. Unfortunately, it is hard to meet the advanced technical requirements of very high efficiency and excellent performances proposed by some cooperative enterprises. To meet the advanced technical requirements, conventional plasma nitriding is necessary to be promoted. It has been reported that titanium-enhanced plasma nitriding has much high efficiency and better performance than that of conventional plasma nitriding. Since Aluminum can react with both nitrogen and iron to form very hard AlN and Fe<sub>x</sub>Al compounds, it can be supposed that Aluminum-enhanced plasma nitriding may have better performances than that of titanium-enhanced plasma nitriding. However, since Aluminum has much lower melting point, Aluminum-enhanced plasma nitriding, also called plasma aluminum-nitriding, can not be conducted by putting Aluminum sheet or particles in the furnace during plasma nitriding, as was performed during titanium-enhanced plasma nitriding. Therefore, the novel method to carry out plasma aluminum-nitriding was primarily explored and developed in this research. And the effect of the novel plasma aluminum-nitriding technology on the efficiency and properties were systematically investigated. The novel plasma aluminum-nitriding in this research was consisted of the following two steps: firstly, Aluminum hydroxide film was deposited on 42CrMo steel by electrolysis; secondly, plasma aluminum-nitriding was carried out at 520 °C/4 h. Meanwhile, conventional plasma nitriding was conducted under the same conditions as a reference. Optical microscope, X-ray diffractometer, Vickers microhardness tester, friction and wear tester and SEM were used to test and analyze the microstructure, phase, hardness and wear resistance of the cross section. The results showed that at the same process parameter of 520 °C/4 h, a multi-layer structure was formed; the thickness of compound layer and effective hardening layer by plasma aluminum-nitriding was significantly higher than that by conventional plasma nitriding. The thickness of compound layer increased from 17.24 μm to 52.13 μm, and the effective diffusion layer increased from 175 μm to 1 050 μm, it was equivalent to 6 times increase in plasma treating efficiency. Meanwhile, AlN and Fe<sub>x</sub>Al phases were formed in the surface layer, which resulted in great enhancement of hardness and wear resistance of the samples, the surface hardness increased from 750HV0.025 to 1 250HV0.025, the friction coefficient decreased from 0.52 to 0.29, the wear rate decreased from 3.22×10<sup>-5</sup> g/(m·N) to 1.21×10<sup>-5</sup> g/(m·N), and the wear marks are obviously reduced. In all, novel plasma aluminum-nitriding technology was primarily developed by using electrolytic aluminum nitrate to generate aluminum hydroxide precipitation on the surface of samples as a pretreatment. Plasma treating efficiency, surface hardness and wear resistance was dramatically enhanced by the novel plasma aluminum-nitriding technology due to the formation of multi-layer structure.

**KEY WORDS:** 42CrMo steel; plasma nitriding; plasma aluminum-nitriding; wear resistance; friction coefficient; electrodeposition

离子渗氮是一种应用较为广泛的化学热处理方法, 具有环保清洁等特点, 可提升工件试样表面硬度及耐磨性<sup>[1-6]</sup>。但是常规离子渗氮处理的保温时间较长, 在工件承受重载冲击或磨损时, 因为化合物层脆性较大, 易在工件表面出现化合物层局部开裂和脱落, 导致零部件性能过早失效, 降低工件预期服役寿命<sup>[7-11]</sup>。

已有的研究表明, 添加微量合金元素可以改善常规离子渗氮渗层组织和性能, 如添加微量硼离子渗氮, 化合物层中可形成高硬度硼化物, 使耐磨性能大幅度提升<sup>[12-15]</sup>; 添加微量硫可在化合物层形成硫化物, 达到减小摩擦因数及提升抗擦伤能力的效果<sup>[16]</sup>; 添加微量钛可改善渗层特性, 提升渗层冲击韧性<sup>[17]</sup>。

基于 Al 可与 N 和 Fe 结合形成性能优良的 AlN 及 Fe<sub>x</sub>Al 相, 特别是 AlN 具有高硬度、高耐磨、低摩

擦因数, 以及磨损时具有自润滑能力, 因此可以预期: 添加微量铝有可能对离子渗氮效果产生显著提升作用<sup>[18-20]</sup>。但是, 由于铝的熔点较低, 无法像其他合金元素一样直接放入离子渗氮炉里, 实现离子氮铝共渗。因此, 设计新型离子共渗试验方法是实现离子氮铝共渗技术的必要手段。

本研究首次探索采用电解硝酸铝生成氢氧化铝沉淀附着在工件表面作为预处理, 进行离子氮铝共渗。目的是研究离子氮铝共渗对 42CrMo 钢组织性能的影响。研究表明, 该方法成功实现了离子氮铝共渗, 且比传统离子渗氮效率和性能都得到显著提高。

## 1 试验

材料使用为调质态 42CrMo 钢, 基体硬度为

370HV0.025, 化学成分(以质量分数计)为: 0.39% C, 0.89% Cr, 0.77% Mn, 0.28% Si, 0.21% Mo, 其余为 Fe。用线切割加工成 10 mm×10 mm×5 mm 的试样, 并采用 180<sup>#</sup>—1500<sup>#</sup>的砂纸逐一进行打磨, 然后将样品放在无水乙醇中用超声波清洗 5 min 去除杂质。采用文献中报道的电解法在试样表面沉积氢氧化铝膜<sup>[21]</sup>, 具体过程为: 将试样接在型号为 ITECH-IT6721 直流电源器阴极, 阳极为纯铝; 然后放入质量浓度为 30 g/L 的硝酸铝溶液中, 调节电流密度为 6 mA/cm<sup>2</sup> 进行电解; 工作电压为 3 V, 工作电流为 0.024 A, 电解时间为 10 min。将沉积氢氧化铝试样取出吹干后放入离子渗氮炉中, 在 520 °C/4 h 下进行离子氮铝共渗。为进行对比研究, 在相同工艺参数(520 °C/4 h)下对 42CrMo 钢进行常规离子渗氮。

等离子处理后, 用 DMI-3000M 型号光学显微镜对工件试样的横截面组织及表面磨痕形貌进行观察。用 D/max-2500 型号 X 射线衍射仪对工件试样物相组成进行测试分析, 使用射线为 Cu-K $\alpha$  射线, 波长  $\lambda=1.54\times 10^{-10}$  m, 扫描速率为 0.2 (°)/min, 其步宽设定为 0.02°, 2 $\theta$  角度为 20°~100°。显微硬度使用型号为 HXD-1000TMC 维氏硬度计对工件横截面硬度进行测量, 载荷为 25 g, 压力保持时间 15 s。用型号为 MMV-1A 多功能材料摩擦磨损测试仪测量工件试样耐磨性。对磨材料用 GCr15 钢球, 直径为 5 mm, 转速为 214 r/min, 使用加载载荷为 200 g, 进行对磨时间为 15 min。用 MST-5000 电子天平对磨损前后质量差进行测量, 计算磨损量。采用 SEM 观察表面形貌。

## 2 结果及分析

### 2.1 氢氧化铝镀膜形貌

图 1 为试样通过电解硝酸铝沉积氢氧化铝膜的表面形貌。从图中可以看出, 在工件表面出现大量微小氢氧化铝碎块, 并且相邻碎块之间存在间隙, 这些间隙可以很好地将溅射到试样表面的氮原子和铝原子吸附在工件表面并向内扩散。

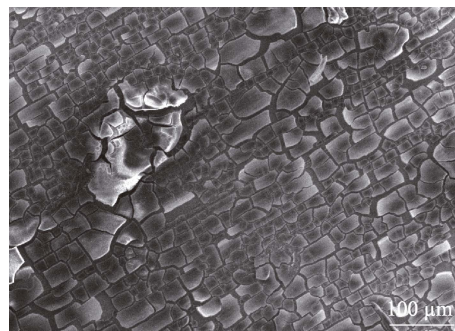


图 1 电解硝酸铝沉积氢氧化铝膜的表面形貌  
Fig.1 Morphology of aluminum hydroxide deposited by electrolytic aluminum nitrate

### 2.2 渗层横截面显微组织

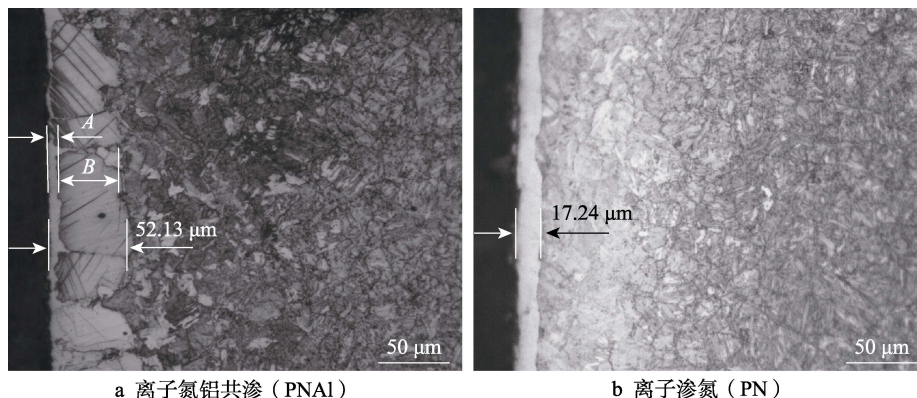
图 2 为相同工艺参数(520 °C/4 h)下等离子处理后试样截面显微组织。可以看出, 离子氮铝共渗(PNAI)处理后, 化合物层显微形貌不同于常规离子渗氮, 形成了图 2a 所示的多层次渗层组织, 如同大锯齿形状牢牢钉在试样基体中, 同时化合物层厚度大幅度提高, 由常规离子渗氮的 17.24 μm 显著增厚到 52.13 μm。

### 2.3 XRD 分析

图 3 为相同工艺参数(520 °C/4 h)下等离子处理后物相分析图(XRD)。从图中可以看出, 离子氮铝共渗(PNAI)处理后出现了 AlN 及 Fe<sub>x</sub>Al 相, 且  $\gamma'$ -Fe<sub>4</sub>N 和  $\epsilon$ -Fe<sub>2-3</sub>N 衍射峰比离子渗氮(PN)时降低, 说明离子氮铝共渗层中  $\gamma'$ -Fe<sub>4</sub>N 和  $\epsilon$ -Fe<sub>2-3</sub>N 含量减少。

### 2.4 截面硬度

图 4 为相同工艺参数(520 °C/4 h)下等离子处理后试样截面硬度。可以看出, 离子氮铝共渗(PNAI)处理后, 试样表层硬度远高于常规离子渗氮(PN)处理, 表面硬度由 750HV0.025 提高到 1 250HV0.025; 有效硬化层由 175 μm 显著增加到 1 050 μm, 相当于等



a 离子氮铝共渗(PNAI)

b 离子渗氮(PN)

图 2 相同工艺参数(520 °C/4 h)下等离子处理后截面显微组织

Fig.2 Cross-sectional microstructure of samples treated by PNAI and PN under the same process parameters: a) PNAI; b) PN

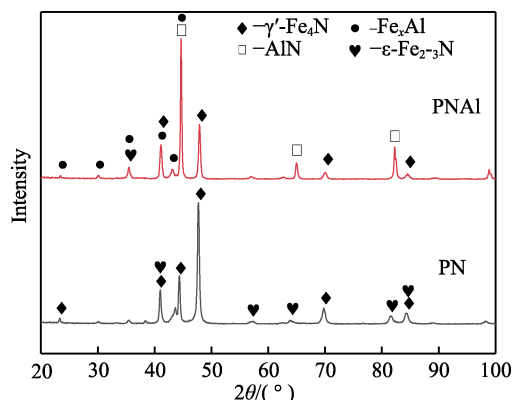


图 3 相同工艺参数 (520 °C/4 h) 下离子氮铝共渗 (PNAI) 和离子渗氮 (PN) 处理后物相分析  
Fig.3 X-ray diffraction patterns of samples treated by PNAI and PN under the same process parameters

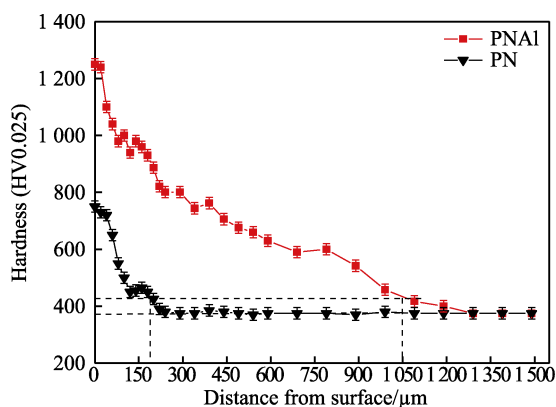


图 4 相同工艺参数 (520 °C/4 h) 下离子氮铝共渗 (PNAI) 和离子渗氮 (PN) 截面硬度  
Fig.4 Micro-hardness profile of samples treated by PNAI and PN under the same process parameters

离子处理效率提升 6 倍。图 4 中可见, 离子氮铝共渗 (PNAI) 和离子渗氮 (PN) 处理后, 表面硬度比基体硬度 375HV0.025 分别提升了 875HV0.025 和 375HV0.025。

## 2.5 耐磨性分析

图 5 为相同工艺参数 (520 °C/4 h) 下等离子处

理后的摩擦因数。可以看出, 离子氮铝共渗处理后, 试样摩擦因数为 0.29, 明显低于常规离子渗氮处理的 0.52, 且离子氮铝共渗处理试样的摩擦因数曲线较平滑, 波动幅度较小。

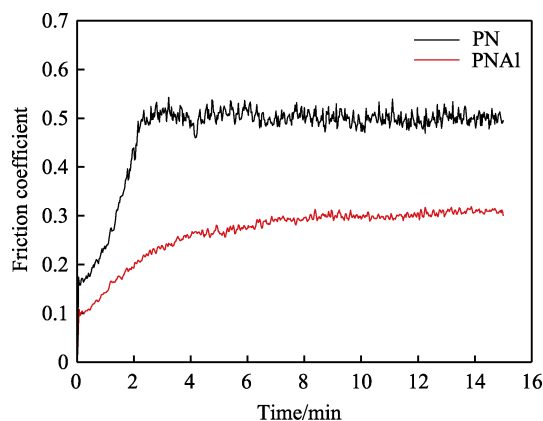


图 5 相同工艺参数 (520 °C/4 h) 下等离子处理后摩擦因数对比

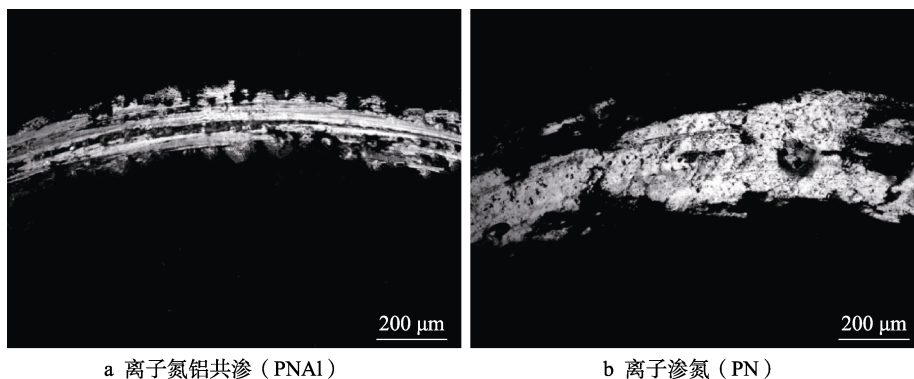
Fig.5 Friction coefficient of samples treated by PNAI and PN under the same process parameters

图 6 为相同工艺参数 (520 °C/4 h) 下等离子处理后的磨痕形貌。可以看出, 离子氮铝共渗试样表面磨损凹坑较小, 只出现较细的磨槽, 且表面破碎痕迹较少。常规离子渗氮试样磨痕较宽, 且磨损表面有较大凹坑和磨损物产生, 导致摩擦因数曲线波动较大, 见图 5。

为进一步评估氮铝共渗与常规离子渗氮试样的耐磨性, 根据式 (1) 所示的比磨损率计算方法<sup>[22]</sup>进行了量化对比分析。

$$W = \Delta m / (NL) \quad (1)$$

式中:  $\Delta m$  为工件磨损前后质量损失差 (g);  $N$  为施加荷载大小 (N);  $L$  为滑动距离 (m)。计算结果如图 7 所示, 从图中可以看出, 氮铝共渗试样磨损率显著降低, 由常规离子渗氮试样的  $3.22 \times 10^{-5} \text{ g}/(\text{m} \cdot \text{N})$  下降到  $1.21 \times 10^{-5} \text{ g}/(\text{m} \cdot \text{N})$ , 即耐磨性提高约 2.7 倍。



a 离子氮铝共渗 (PNAI)

b 离子渗氮 (PN)

图 6 相同工艺参数 (520 °C/4 h) 下等离子处理后磨痕形貌对比  
Fig.6 Morphology of wear mark of samples treated by PNAI and PN under the same process parameters: a) PNAI; b) PN



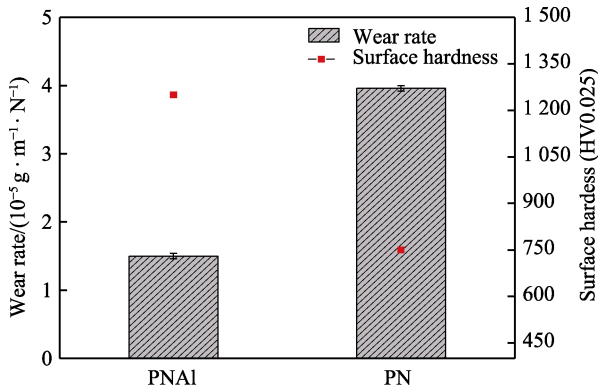
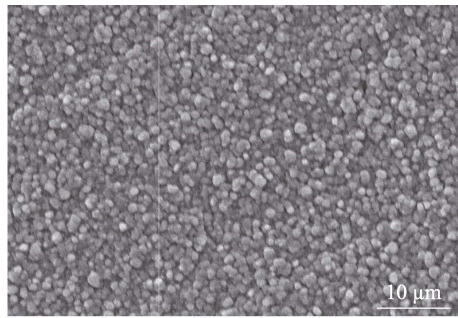


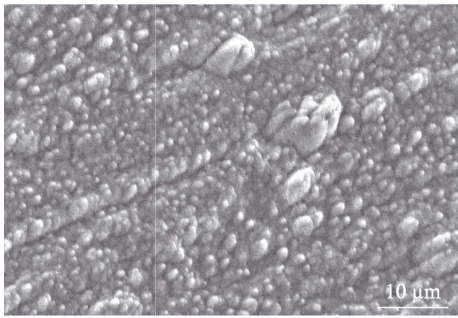
图 7 相同工艺参数 (520 ℃/4 h) 下等离子处理后磨损率与表面硬度对比  
Fig.7 Wear rate of samples treated by PNAI and PN under the same process parameters

2.6 表面 SEM-EDS 分析

试样在相同工艺参数 (520 ℃/4 h) 下等离子处理后的表面形貌见图 8。可见, 离子氮铝共渗 (图 8a)



a 离子氮铝共渗 (PNAI)



b 离子渗氮 (PN)

图 8 相同工艺参数 (520 ℃/4 h) 下等离子处理后试样表面形貌及元素含量 (SEM-EDS)  
Fig.8 SEM-EDS of samples treated by PNAI and PN under the same process parameters: a) PNAI; b) PN

后表面颗粒不但细小且均匀, 表面粗糙度相对于常规离子渗氮较小; 而常规离子渗氮 (图 8b) 后表面颗粒均匀性较差, 且存在大颗粒突起, 这些较大的突起相当于坚硬磨粒, 会导致摩擦因数的波动性较大, 见图 4。在磨损过程中会从黏着磨损变成为磨粒磨损, 这将显著增加对磨材料与样品间的磨损程度, 导致试样表面在磨损时形成大量拉伤及划伤, 使耐磨性大幅降低<sup>[23-25]</sup>, 见图 5。表面元素含量 EDS 分析结果见表 1—2, 可见, 离子氮铝共渗后表面铝元素含量达到 10.32%; 同时氮元素含量由常规离子渗氮 12.53% 提升到 16.93%, 表面氮浓度的提高可能源于强氮化物形成元素铝的吸引效果, 高氮浓度有利于渗层的快速形成。

表 1 离子氮铝共渗 EDS 元素分布  
Tab.1 EDS element distribution after PNAI

| Element | wt. % | at. % |
|---------|-------|-------|
| N       | 16.93 | 40.6  |
| Al      | 10.32 | 12.8  |
| Fe      | 72.75 | 43.6  |
| Total   | 100   | 100   |

表 2 常规离子渗氮 EDS 元素分布  
Tab.2 EDS element distribution after PN

| Element | wt. % | at. % |
|---------|-------|-------|
| N       | 12.53 | 36.4  |
| Fe      | 87.47 | 63.6  |
| Total   | 100   | 100   |

3 分析与讨论

离子氮铝共渗与常规离子渗氮试样组织性能对比总结见表 3。可见, 试样离子氮铝共渗 (PNAI) 处理的效率、表层硬度及耐磨性都远远优于常规离子渗氮 (PN) 处理, 且表面形成了图 8 所示的细小均匀分布的微米颗粒。

高性能离子氮铝共渗层高效形成机理可能是: 沉积在试样表面的微小块状  $\text{Al}(\text{OH})_3$  之间产生大量微裂纹, 极大地提升了试样表面粗糙度, 有利于吸附轰击试样的氮原子, 提高氮原子浓度, 使氮原子扩散能力

表 3 离子氮铝共渗与常规离子渗氮对比  
Tab.3 Comparative study of the characteristics of PNAI and PN layer

| Characteristics of treated layer                  |  | PNAI  | PN  | PNAI vs. PN                                 |
|---|--|---|---|---|
| Compound layer thickness/ $\mu\text{m}$           |  | 52.13   | 17.24   | 200%↑                                       |
| Effective hardened layer thickness/ $\mu\text{m}$ |  | 1 050   | 175   | 500%↑                                       |
| Surface hardness (HV0.025)                        |  | 1 250   | 750   | 67%↑  |
| Wear resistance                                   | Wear rate/ $(10^{-5} \text{ g} \cdot \text{m}^{-1} \cdot \text{N}^{-1})$ | 1.21  | 3.22  | 166%↓                                       |
|   | Friction coefficients  | 0.29  | 0.52  | 79%↓  |
| Main phases of nitriding layer                    |  | $\text{Fe}_x\text{Al}$ , $\text{AlN}$ , $\text{Fe}_{2-3}\text{N}$ , $\text{Fe}_4\text{N}$ | $\text{Fe}_{2-3}\text{N}$ , $\text{Fe}_4\text{N}$ | Added $\text{Fe}_x\text{Al}$ , $\text{AlN}$ |

提升<sup>[26-27]</sup>。Al(OH)<sub>3</sub> 在高温时分解成孔缝状 Al<sub>2</sub>O<sub>3</sub> 和游离态 H<sub>2</sub>O; 游离态 H<sub>2</sub>O 与 Fe 反应生成 Fe<sub>3</sub>O<sub>4</sub>, 从而在工件表面形成孔洞, 孔缝状 Al<sub>2</sub>O<sub>3</sub> 和氧化孔洞都为氮原子扩散提供大量通道<sup>[28]</sup>, 从而提高氮原子扩散速率, 加速白亮层形成; 使离子氮铝共渗层硬度显著高于传统离子渗氮。同时, 因离子氮铝共渗处理后渗层中形成了图 2 所示的高硬度 AlN 及 Fe<sub>x</sub>Al 相<sup>[29-30]</sup>, 使表面硬度及有效硬化层显著提高。

## 4 结论

1) 离子氮铝共渗处理比常规离子渗氮效率明显提高, 化合物层厚度由 17.24 μm 增加到 52.13 μm, 有效扩散层从 175 μm 增加到 1 050 μm, 相当于离子处理效率提升约 6 倍。

2) 离子氮铝共渗处理后渗层中形成了高硬度 AlN 及 Fe<sub>x</sub>Al 相, 且表面颗粒细小均匀分布。

3) 离子氮铝共渗处理后表面硬度由常规离子渗氮的 750HV0.025 提高至 1 250HV0.025, 提升了 500HV0.025。离子氮铝共渗处理和离子渗氮处理后, 表面硬度比基体硬度 375HV0.025 分别提升了 875HV0.025 和 375HV0.025。

4) 离子氮铝共渗处理后试样表面的耐磨性显著提高, 摩擦因数由常规离子渗氮的 0.52 下降到 0.29; 磨痕较浅较窄; 磨损率由  $3.22 \times 10^{-5}$  g/(m·N) 下降到  $1.21 \times 10^{-5}$  g/(m·N), 相当于耐磨性提高到常规离子渗氮的 2.7 倍。

## 参考文献:

- [1] LIU Han, LI Jing-cai, CHAI Ya-ting, et al. A Novel Plasma Oxynitriding by Using Plain Air for AISI 1045 Steel[J]. Vacuum, 2015, 121: 18-21.
- [2] 唐磊, 陈尧, 彭甜甜, 等. H13 热冲压模具无化合物层抗冲击抗热疲劳离子渗氮技术研究与应用[J]. 表面技术, 2018, 47(11): 48-53.  
TANG Lei, CHEN Yao, PENG Tian-tian, et al. Study and Application of Non-Compound Layer Plasma Nitriding with Impact and Thermal Fatigue Resistance for H13 Hot Stamping Die Steel[J]. Surface Technology, 2018, 47(11): 48-53.
- [3] BELL T, SUN Y, SUHADI A. Environmental and Technical Aspects of Plasma Nitrocarburising[J]. Vacuum, 2000, 59(1): 14-23.
- [4] CASTELETTI L C, NETO A L, TOTTEN G E. Nitriding of Stainless Steels[J]. Metallography, Microstructure, and Analysis, 2014, 3(6): 477-508.
- [5] 李杨, 何永勇, 朱宜杰, 等. 2Cr13 马氏体不锈钢活性屏离子渗氮技术[J]. 金属热处理, 2017, 42(5): 163-167.  
LI Yang, HE Yong-yong, ZHU Yi-jie, et al. Active Screen Plasma Nitriding of 2Cr13 Martensitic Stainless Steel[J]. Heat Treatment of Metals, 2017, 42(5): 163-167.
- [6] 彭甜甜, 林超林, 陈尧, 等. 离子渗氮化合物层相调控对耐磨性的影响[J]. 表面技术, 2020, 49(8): 172-177.  
PENG Tian-tian, LIN Chao-lin, CHEN Yao, et al. Effect of Phase Regulation of Plasma Nitriding Compound Layer on Wear Resistance[J]. Surface Technology, 2020, 49(8): 172-177.
- [7] 卢世静, 孙斐, 缪小吉, 等. 离子渗氮和固溶复合处理制备深层含氮奥氏体不锈钢[J]. 表面技术, 2018, 47(10): 180-185.  
LU Shi-jing, SUN Fei, MIAO Xiao-ji, et al. Preparation for Deep Nitriding Austenitic Stainless Steel by Complex Treatment of Plasma Nitriding and Solid Solution[J]. Surface Technology, 2018, 47(10): 180-185.
- [8] KIM Y M, SON S W, LEE W B. Thermodynamic and Kinetic Analysis of Formation of Compound Layer during Gas Nitriding of AISI1018 Carbon Steel[J]. Metals and Materials International, 2018, 24(1): 180-186.
- [9] SAEED A, KHAN A W, JAN F, et al. Optimization Study of Pulsed DC Nitrogen-Hydrogen Plasma in the Presence of an Active Screen Cage[J]. Plasma Science and Technology, 2014, 16(5): 460-464.
- [10] 麻恒, 赵晓兵, 魏坤霞, 等. 42CrMo<sub>4</sub> 钢硼氮离子复合渗与离子渗氮对比研究[J]. 表面技术, 2022, 51(4): 121-126.  
MA Heng, ZHAO Xiao-bing, WEI Kun-xia, et al. Comparative Study on Plasma Boron-Nitriding and Plasma Nitriding for 42CrMo<sub>4</sub> Steel[J]. Surface Technology, 2022, 51(4): 121-126.
- [11] NISHIMOTO A, NAGATSUKA K, NARITA R, et al. Effect of the Distance between Screen and Sample on Active Screen Plasma Nitriding Properties[J]. Surface and Coatings Technology, 2010, 205: S365-S368.
- [12] MA Heng, WEI Kun-xia, ZHAO Xiao-bing, et al. Performance Enhancement by Novel Plasma Boron-Nitriding for 42CrMo<sub>4</sub> Steel[J]. Materials Letters, 2021, 304: 130709.
- [13] LI Jing-cai, YANG Xing-mei, WANG Shu-kai, et al. A Rapid D.C. Plasma Nitriding Technology Catalyzed by Pre-Oxidation for AISI4140 Steel[J]. Materials Letters, 2014, 116: 199-202.
- [14] 李景才, 孙斐, 王树凯, 等. 离子渗氮前预氧化催渗作用及机理[J]. 材料热处理学报, 2014, 35(7): 182-186, 192.  
LI Jing-cai, SUN Fei, WANG Shu-kai, et al. Catalysis Effect and Mechanism of Pre-Oxidation on Direct Current Plasma Nitriding[J]. Transactions of Materials and Heat Treatment, 2014, 35(7): 182-186, 192.
- [15] NAEEM M, TORRES A V R, SERRA P L C, et al. Combined Plasma Treatment of AISI-1045 Steel by Hastelloy Deposition and Plasma Nitriding[J]. Journal of Building Engineering, 2022, 47: 103882.
- [16] 王海斗, 庄大明, 王昆林, 等. 不同钢种离子渗氮层的抗擦伤性能研究[J]. 材料工程, 2003, 31(2): 7-10.  
WANG Hai-dou, ZHUANG Da-ming, WANG Kun-lin, et

- al. Study on Anti-Scuffing Properties of Ion Sulfide Layers under Oil Lubrication[J]. Journal of Materials Engineering, 2003, 31(2): 7-10.
- [17] 毛长军, 魏坤霞, 刘细良, 等. 微量钛对离子渗氮渗层特性及性能的影响[J]. 中国表面工程, 2020, 33(1): 34-38.
- MAO Chang-jun, WEI Kun-xia, LIU Xi-liang, et al. Effects of Trace Titanium on Characteristics and Properties of Plasma Nitriding Layer[J]. China Surface Engineering, 2020, 33(1): 34-38.
- [18] BINDUMADHAVAN P N, MAKESH S, GOWRISH-ANKAR N, et al. Aluminizing and Subsequent Nitriding of Plain Carbon Low Alloy Steels for Piston Ring Applications[J]. Surface and Coatings Technology, 2000, 127(2-3): 251-258.
- [19] TANG Ming-qi, WANG Jian-feng, FENG Zai-qiang, et al. Corrosion Resistance of AlN and Fe<sub>3</sub>Al Reinforced Fe-Based Plasma Cladding Layer in 3.5 wt% NaCl Solution[J]. Ceramics International, 2019, 45(14): 16918-16926.
- [20] GEDAM V, PANSARI A, SINHA A K, et al. The Effect of Macroscopic Polarization on Intrinsic and Extrinsic Thermal Conductivities of AlN[J]. Journal of Physics and Chemistry of Solids, 2015, 78: 59-64.
- [21] 陶涛, 陈启元, 李元高, 等. 铝酸钠溶液离子膜电解方法制备氢氧化铝[J]. 中南大学学报(自然科学版), 2007, 38(1): 102-106.
- TAO Tao, CHEN Qi-yuan, LI Yuan-gao, et al. Production of Al(OH)<sub>3</sub> by Ion Membrane Electrolysis in Sodium Aluminate Solution[J]. Journal of Central South University (Science and Technology), 2007, 38(1): 102-106.
- [22] WANG Y X, YAN M F, LI B, et al. Surface Properties of Low Alloy Steel Treated by Plasma Nitrocarburizing Prior to Laser Quenching Process[J]. Optics & Laser Technology, 2015, 67: 57-64.
- [23] REN Yan-ping, WANG Peng-fei, CAI Zhen-bing, et al. Dynamic Response Characteristics and Damage Mechanism of Impact Wear for Deep Plasma Nitrided Layer[J]. Tribology International, 2022, 170: 107496.
- [24] WANG Bo, ZHAO Xing-feng, LI Wen-zheng, et al. Effect of Nitrided-Layer Microstructure Control on Wear Behavior of AISI H13 Hot Work Die Steel[J]. Applied Surface Science, 2018, 431: 39-43.
- [25] 陈尧, 宋磊, 张宸恺, 等. 38CrMoAl 液压柱塞无白亮层低温离子渗氮工艺研究[J]. 机械工程学报, 2017, 53(22): 81-86.
- CHEN Yao, SONG Lei, ZHANG Chen-kai, et al. Lower Temperature Plasma Nitriding without White Layer for 38CrMoAl Hydraulic Plunger[J]. Journal of Mechanical Engineering, 2017, 53(22): 81-86.
- [26] 李双喜, 李宝奎, 李晓丹, 等. 温度和表面粗糙度对 40CrNiMo 钢离子渗氮的影响[J]. 金属热处理, 2019, 44(6): 201-203.
- LI Shuang-xi, LI Bao-kui, LI Xiao-dan, et al. Effect of Temperature and Surface Roughness on Plasma Nitriding of 40CrNiMo Steel[J]. Heat Treatment of Metals, 2019, 44(6): 201-203.
- [27] SINGH G P, ALPHONSA J, BARHAI P K, et al. Effect of Surface Roughness on the Properties of the Layer Formed on AISI 304 Stainless Steel after Plasma Nitriding[J]. Surface and Coatings Technology, 2006, 200(20-21): 5807-5811.
- [28] MADANIPOUR H, SOLTANIEH M, NAYEBPASHAEE N. Investigation of the Formation of Al, Fe, N Inter-metallic Phases during Al Pack Cementation Followed by Plasma Nitriding on Plain Carbon Steel[J]. Materials & Design, 2013, 51: 43-50.
- [29] PARK J K, BAIK Y J. Increase of Hardness and Oxidation Resistance of VN Coating by Nanoscale Multilayered Structurization with AlN[J]. Materials Letters, 2008, 62(16): 2528-2530.
- [30] PENG Jia-wan, ZHANG Feng-lin, HUANG Yao-jie, et al. Comparative Study on NiAl and FeAl Intermetallic-Bonded Diamond Tools and Grinding Performance for Si<sub>3</sub>N<sub>4</sub> Ceramic[J]. Ceramics International, 2021, 47(23): 32736-32746.

责任编辑: 万长清